

# Detection of HI 21cm Absorption by the Warm Neutral Medium

C.L. Carilli

National Radio Astronomy Observatory, P.O. Box O, Socorro, NM, 87801

K.S. Dwarakanath

Raman Research Institute, Bangalore 560 080, India

W.M. Goss

National Radio Astronomy Observatory, P.O. Box O, Socorro, NM, 87801

Received \_\_\_\_\_; accepted \_\_\_\_\_

To appear in the Astrophysical Journal (letters)

## ABSTRACT

We have detected HI 21cm line absorption by the Warm Neutral Medium (WNM) using the Westerbork Synthesis Radio Telescope. The absorption was detected toward Cygnus A at LSR velocities of  $-40$  and  $-70$  km s $^{-1}$ . These two velocity ranges were previously identified as being relatively free of cold absorbing clouds. The measured optical depth for the WNM along the line of sight to Cygnus A is  $8.9 \pm 1.9 \times 10^{-4}$  at  $-70$  km s $^{-1}$ , and  $8.5 \pm 2.0 \times 10^{-4}$  at  $-40$  km s $^{-1}$ , with corresponding spin temperatures of  $6000 \pm 1700$  K and  $4800 \pm 1600$  K, respectively. The volume filling factor for the WNM appears to be fairly high ( $f \approx 0.4$ ).

*Subject headings: ISM: structure and atoms – Galaxy: fundamental parameters – Radio Lines: ISM*

## 1. Introduction

Early observations of the 21cm line of neutral hydrogen in emission and absorption in the Galaxy showed that toward any given direction the HI line seen in emission was always broader than the corresponding HI absorption line. In addition, most lines of sight showed a broad HI emission line with no corresponding HI absorption (Clark, Radhakrishnan, & Wilson 1962, Clark 1965, Radhakrishnan et al. 1972). These observations led to the proposal of a ‘raisin-pudding’ model of the interstellar medium (Field, Goldsmith, & Habing 1969), in which dense cool HI clouds at  $10^2$  K (the Cold Neutral Medium; CNM) are enveloped by a warmer, lower density gas at  $10^4$  K (the Warm Neutral Medium; WNM). More recent models for the interstellar medium include a high filling factor, Hot Ionized Medium (HIM) at  $10^6$  K, resulting from supernovae explosions (McKee and Ostriker 1977). The phases of the interstellar medium are thought to be in pressure equilibrium, although the relative filling factors of the different phases remain uncertain, and the filling factors may vary with position in galaxies (Brinks 1990, Braun and Walterbos 1992).

Kulkarni and Heiles (1988) point out that of all the phases of the interstellar medium (ISM), the WNM remains the least well understood. Although HI 21cm emission from the WNM is detected easily in every direction in the sky, an accurate value for the temperature of the WNM is lacking. The standard method with which to determine the temperature of interstellar HI is to compare HI column densities determined by observation of the 21cm line in emission in a given region, with those determined by observation of 21cm absorption towards background continuum sources (Clark 1965). The result is the excitation, or spin temperature, of the gas. The spin temperature,  $T_s$ , is thought to be close to the kinetic temperature in most Galactic environments. There are three well known problems with this method. The first is that one has to interpolate HI column densities determined off-source to the position of the continuum source. For the WNM this is not a severe problem, since

the column density distribution appears to be fairly smooth on scales  $\geq 10'$  (Kalberla, Schwarz, and Goss 1985). Second, when looking for absorption by the WNM, there is the confusion caused by the plethora of absorption lines arising in the CNM. And third, there is the problem of having both emission and absorption in the on-source beam, and the related problem of ‘stray-radiation’, or emission coming in through the sidelobes of the telescope beam. This is especially a problem for single dish observations, for which beam sizes are typically much larger than the background continuum sources.

Kulkarni and Heiles (1988) review measurements of the temperature of the WNM. They conclude that the current data, which entails mostly lower limits to  $T_s$ , are consistent with a temperature range of 5000 K to 8000 K for most of the WNM. They emphasize that the current data are sparse, and that ‘observational confirmation of this conclusion is *crucial*.’ The single existing experiment claiming detection of absorption by the WNM is that by Mebold and Hills (1975). They studied HI emission and absorption in the vicinity of the bright extragalactic radio source Cygnus A using the Effelsberg 100 m telescope. Their experiment consisted of eight off-source pointings encircling the continuum source, to determine the HI column density distribution in the region, and on-source observations to look for absorption. They found two inter-arm velocity ranges with no narrow absorption features due to the CNM. At these velocities their on-source spectrum of Cygnus A shows HI in *emission*, however, the amount of emission seen on-source is less than that expected from the interpolation of the off-source pointings to the source position. From this they *infer* absorption towards the continuum source. Mebold and Hills estimate an optical depth for the WNM between  $6 \times 10^{-4}$  and  $11 \times 10^{-4}$ , and a spin temperature between 6400 K and 7800 K. Kalberla, Mebold, and Reich (1980) re-analyzed these data, correcting for stray radiation, and reduced the spin temperature estimates by about 20%.

In this letter we present a direct verification of absorption toward Cygnus A in the

CNM-free velocity ranges using the Westerbork Synthesis Radio Telescope (WSRT). We then derive the spin temperature for the WNM in the two CNM-free velocity ranges using the WSRT absorption measurements and emission spectra from the Effelsberg and Dwingeloo telescopes. We discuss these results in terms of standard equilibrium models for the two-phase neutral atomic ISM.

## 2. Observations of CNM-free Regions toward Cygnus A

The CNM-free LSR velocity ranges toward Cygnus A are from  $-40$  to  $-36$   $\text{km s}^{-1}$ , and  $-63$  to  $-78$   $\text{km s}^{-1}$ , corresponding to inter-arm velocities, between the Orion ( $0$   $\text{km s}^{-1}$ ), Perseus ( $-50$   $\text{km s}^{-1}$ ), and Outer ( $-85$   $\text{km s}^{-1}$ ) spiral arms (Mebold and Hills 1975). We have searched for absorption by the WNM at these inter-arm velocities using the WSRT. Using an interferometer mitigates problems of confusion by stray radiation and in-beam emission. Observations were made on May 24 and 25, 1996, July 15 and 16, 1996, June 28 and 29, 1997, and August 22 and 23, 1997, for 12 hours each day. The total bandwidth was 1.25 MHz with 255 spectral channels after Hanning smoothing, corresponding to  $1$   $\text{km s}^{-1}$  velocity resolution, centered at an LSR velocity of  $-45$   $\text{km s}^{-1}$ . Absolute flux calibration and initial phase calibration were performed using 3C 286, and residual phase errors were corrected through self-calibration using a continuum data set made from line-free channels.

An accurate bandpass was determined using frequency switching to ‘high’ and ‘low’ frequencies by  $\pm 1.25$  MHz on Cygnus A itself. The cycle time for bandpass calibration was two hours, with a 50% duty cycle, and the bandpass for each cycle was the average of the high and low frequency settings. An estimate of the accuracy of the bandpass calibration process was obtained by applying the ‘high’ frequency bandpass solutions to the ‘low’ frequency spectra. The residual fractional deviations were generally  $\leq 1.7 \times 10^{-4}$ . We adopt this value as a conservative estimate of optical depth errors introduced by the bandpass

calibration process.

The visibility data from each day’s observation were reduced independently using the Astronomical Image Processing System (AIPS). The continuum emission was subtracted using the AIPS task UVLIN, which performs a linear fit to the line-free channels for each visibility, and the data from the eight days were then combined. Spectral line image ‘cubes’ were constructed from the combined data, and the point response function of the array deconvolved, using the AIPS task IMAGR. The Gaussian restoring CLEAN beam had a  $\text{FWHM} = 30'' \times 15''$  with a major axis oriented north-south.

The continuum image of Cygnus A made from line-free channels is shown in Figure 1. The observed total flux density at 1.4 GHz for Cygnus A was within 2% of the expected value of 1575 Jy (Baars et al. 1977). The source is characterized by two ‘hot spots’ of emission at the source extremities, separated by  $2'$ , with a low frequency ‘bridge’ of emission connecting the two hot spots. In the following section we analyze spectra taken at the the Northwest (NW) and Southeast (SE) hot spots. The peak surface brightness is 346 Jy  $\text{beam}^{-1}$  for the NW hot spot and 398 Jy  $\text{beam}^{-1}$  for the SE hot spot.

The HI absorption spectra toward the SE and NW peaks of Cygnus A are shown in Figure 2. The spectra show deep, narrow lines due to the CNM, clustered around the spiral arm velocities (0,  $-50$ , and  $-85 \text{ km s}^{-1}$ ), with optical depths approaching 0.5. There are significant variations in optical depth for these narrow lines between the two lines of sight separated by  $2'$ . Small scale structure in the CNM is a well studied phenomenon (Dieter et al. 1976, Diamond et al. 1989, Deshpande et al. 1992, Frail et al. 1994, Davis, Diamond, and Goss 1996), and a detailed analysis of the CNM structure toward Cygnus A will be presented elsewhere. The root mean square (rms) noise per channel in these spectra is 0.1 mJy  $\text{channel}^{-1}$ , corresponding to an rms optical depth ( $\sigma$ ) of about  $2.5 \times 10^{-4}$  per channel.

Note the lack of deep, narrow absorption features in the inter-arm velocity ranges from

–40 to –36 km s<sup>–1</sup> (region ‘B’ in the spectra), and –63 to –78 km s<sup>–1</sup> (region ‘A’), as first pointed out by Mebold and Hills (1975). Figures 3 & 4 show these same spectra with an expanded flux and optical depth scale in order to investigate possible absorption in these two CNM-free velocity ranges. The observed (continuum subtracted) surface brightnesses in regions A and B appear to be significantly below zero in all the spectra. The mean optical depth values in regions A and B are listed in Table 1. The errors are a (quadratic) sum of the sensitivity error (ie. the rms in off-line channels after averaging over the specified number of channels), and the estimated error due to bandpass calibration.

The optical depth in velocity region B is marginally higher toward the SE source relative to the NW source ( $1.8\sigma$ ). However the SE source spectrum shows a narrow absorption line by the CNM at –30 km s<sup>–1</sup> which is not seen toward the NW source. The wing of this line might perturb the measured value in region B. Similarly, the spectrum of the SE component in velocity region A shows what might be a narrow, weak absorption component at –69 km s<sup>–1</sup>. In the analysis below we use the optical depths in regions A and B averaged over both SE and NW spectra (row three in Table 1), with errors as dictated by each measurement.

We are confident that the finite optical depths observed at the CNM-free velocities are reliable for a number of reasons. First, the observed optical depths are significantly higher than the estimated accuracy of the bandpass calibration. Second, we have analyzed spectra from data taken from the four epochs separately (May and July 1996, and June and August 1997), and obtain consistent results for each epoch. And third, we have fit Gaussian models to the strong absorption lines nearest in velocity to the CNM-free regions, and we find that the finite optical depths seen in these regions are not due to the wings of the strong lines. We should emphasize that we cannot rule-out a model in which the finite optical depth seen at the CNM-free velocities toward Cygnus A are due to a ‘continuum’ of low optical depth

cold clouds. If this were the case, the optical depths quoted in Table 1 would be strictly upper limits to the true optical depth of the WNM, and the spin temperature values quoted below then become lower limits.

### 3. Discussion

We can combine our measurement of the HI 21cm optical depth of the WNM with the emission measurements of Mebold and Hills (1975) to obtain a lower limit to the spin temperature of the WNM, using the low-optical depth approximation:  $T_B = \tau T_s$ , where  $\tau$  is the optical depth to 21cm absorption, and  $T_B$  is the brightness temperature of the 21cm emission in the absence of absorption.

One measurement of the emission spectrum in the direction of Cygnus A is the Effelsberg 100m spectrum of Mebold and Hills (1975), which entailed the average of eight emission profiles taken at distances of 20' from Cygnus A in a symmetric star pattern centered on Cygnus A. The brightness temperatures in velocity ranges A and B are given in row four of Table 1. These are the values of Mebold and Hills reduced by 20% to correct for stray radiation (Kalberla et al. 1980). Mebold and Hills quote an error of 1 K for these measurements. A second measurement is from the all-sky HI survey of Hartmann and Burton (1997), using the Dwingeloo 25m telescope, and corrected for stray radiation. The Dwingeloo values are given in row five of Table 1, where we have averaged four measurements surrounding Cygnus A at distances of about 20'. The errors represent the scatter in the measurements. Although the resolutions of the two observations are different (11' for Effelsberg and 30' for Dwingeloo), the  $T_B$  values agree to within the errors. For the calculation of spin temperatures we use the (error weighted) mean  $T_B$  values listed in row six of Table 1. The resulting spin temperature values for velocity regions A and B are listed in row seven of Table 1, where the errors are a quadrature sum of errors on the brightness



temperature measurement and the optical depth measurement.

The Galactic coordinates for Cygnus A are  $l = 76^\circ$ ,  $b = 5.8^\circ$ . The implied distances to the gas in velocity ranges A and B are about 12 kpc and 9 kpc, respectively, as derived from the Galactic rotation curve of Burton (1988). The height of this gas from the plane,  $z$ , is then:  $z \approx 1$  kpc. A very rough estimate of the pathlength through the gas can be derived by assuming that the velocity ranges are set by Galactic rotation, leading to 0.9 kpc and 0.4 kpc for A and B, respectively. Then using the HI column densities calculated from Table 1 leads to a mean density for the WNM in velocity ranges A and B toward Cygnus A of:  $\langle n_{wnm} \rangle \approx 0.03 \text{ cm}^{-3}$ . The ISM pressure at  $z = 1$  kpc is thought to be about  $5 \times 10^{-14} \text{ dyne cm}^{-2}$  (Kulkarni and Heiles 1988, equ. 3.30). This pressure, coupled with the mean temperature of 5400 K for the WNM from Table 1, leads to a density of:  $n_{wnm} = 0.07 \text{ cm}^{-3}$ . Hence the volume filling factor,  $f$ , for the WNM at  $z = 1$  kpc is:  $f \equiv \frac{\langle n_{wnm} \rangle}{n_{wnm}} \approx 0.4$ . This value of  $f$  is consistent with the estimate of Kulkarni and Heiles (1988) of  $f = 0.6$  for the sum of the warm neutral and warm ionized medium, with the dominant component being the WNM in the case where magnetic fields and cosmic ray pressures are substantial. While the uncertainties in the above calculation are significant (in particular the use of small velocity gradients to derive pathlengths), the general implication is that the volume filling factor for the WNM appears to be fairly high.

The HI spin temperature is thought to be driven to the kinetic temperature of the gas through the process of resonant scattering of ambient Ly  $\alpha$  photons (Field 1958). This process depends critically on the local Ly $\alpha$  photon density, which in turn depends on the ionization rate due to cosmic rays and soft X-rays since the HI is opaque to external Ly $\alpha$  photons. Based on the analysis of Galactic low density regions by Deguchi and Watson (1985), Kulkarni and Heiles (1988) state that ‘the ionization rate is large enough in the Galactic environment to make the spin temperature ( $T_s$ )  $\approx$  kinetic temperature ( $T_k$ ) for

almost any HI cloud observable in the 21 cm line.’ The current limit to the diffuse Galactic Ly  $\alpha$  photon density in the solar neighborhood is:  $n_{Ly\alpha} < 2.5 \times 10^{-6} \text{ cm}^{-3}$  (Holberg 1986). This limit is sufficient to maintain  $T_s \approx T_k$  in the WNM if  $T_k \sim 3000 \text{ K}$  (Field 1958). If the value of  $n_{Ly\alpha}$  is considerably below  $10^{-6} \text{ cm}^{-3}$  in the WNM, then  $T_s$  could fall significantly below  $T_k$ . For example, Corbelli and Salpeter (1993) find that temperature equilibrium between  $T_s$  and  $T_k$  may not hold in the outer disks of spiral galaxies, where  $N(\text{HI}) \leq \text{few} \times 10^{19}$ , if the only source of ionizing radiation is the extragalactic background. Until a direct measurement of  $n_{Ly\alpha}$  in the WNM becomes available, we can only assume that  $T_s \approx T_k$  in the disk of the Galaxy.

The most detailed analysis of the equilibrium state of neutral hydrogen in the interstellar medium is the work of Wolfire et al. (1995). The primary heating mechanism is photoelectric emission from dust grains, while cooling is dominated by fine structure lines from heavy elements (predominantly Carbon), and by hydrogen recombination lines in warmer regions. In their standard model for neutral hydrogen in the Galactic plane they show that two stable phases exist: (i) the CNM with  $T_k$  between 40 K and 200 K, and (ii) the WNM with  $T_k$  between 5500 K and 8700 K, for ISM pressures in the range of 1 to  $5 \times 10^{-13} \text{ dyne cm}^{-2}$ . It is interesting that the measured values of  $T_s$  in the lower pressure (ie. larger  $z$ ) WNM toward Cygnus A (Table 1) are generally consistent with these ranges for the neutral, two-phase ISM model of Wolfire et al. (1995). Corbelli and Salpeter (1993) point out that equality between  $T_s$  and  $T_k$  could be used to argue that the ionizing radiation field for the WNM is well above the extragalactic background, and hence that ‘relevant energy inputs from local sources become necessary.’ While the current data toward Cygnus A are consistent with the value of  $T_s$  being close to the model value of  $T_k$  for the WNM, more accurate values for  $T_s$  and  $T_B$  for the neutral hydrogen, and  $n_{Ly\alpha}$ , are needed to provide a fully constrained physical model for the Galactic WNM.

The National Radio Astronomy Observatory (NRAO) is a facility of the National Science Foundation, operated under cooperative agreement by Associated Universities, Inc.. The Westerbork Synthesis Radio Telescope is operated by the Netherlands Foundation for Research in Astronomy with financial support from the Netherlands Organization for Scientific Research (NWO). We wish to thank K. Anantharamiah, W.B. Burton, A.A. Deshpande, G. Field, D. Hartmann, C. Heiles, S. Kulkarni, U. Mebold, G. Srinivasan, and the referee for useful comments on this work.

## References

- Baars, J., Genzel, R., Pauliny-Toth, I., and Witzel, A. 1977, *A&A*, 61, 99.
- Braun, R. and Walterbos, R. 1992 *Ap.J.*, 386, 120
- Brinks, E. 1990, in *The Interstellar Medium in Galaxies*, eds. H.A. Thronson and J.M. Shull (Dordrecht: Kluwer), p. 39.
- Burton, W. Butler 1988, in *Galactic and Extragalactic Radio Astronomy*, eds. G. Verschuur and K. Kellerman (Heidelberg: Springer-Verlag), p. 295
- Clark, B. G. 1965, *ApJ*, 142, 1398.
- Clark, B. G., Radhakrishnan, V., & Wilson, R. W. 1962, *ApJ*, 135, 151.
- Corbelli, E. and Salpeter, E.E. 1993, *Ap.J.*, 419, 94
- Davis, R.J., Diamond, P.J., and Goss, W.M. 1996, *MNRAS*, 283, 1105
- Deguchi, S. and Watson, W.D. 1985, *Ap.J.*, 290, 578
- Deshpande, A. A., McCulloch, P. M., Radhakrishnan, V., & Anantharamaiah, K. R. 1992, *MNRAS*, 258, 19p.
- Diamond, P. J., Goss, W. M., Romney, J. D., Booth, R. S., Kalberla, P. M. W., & Mebold, U. 1989, *ApJ*, 347, 302.
- Dieter, N. H., Welch, W. J., & Romney, J. D. 1976, *ApJ*, 206, L113.
- Field, G. B. 1958, *Proc. IRE*, 46, 240.
- Field, G. B., Goldsmith, D. W., & Habing, H. J. 1969, *ApJ*, 155, L149.
- Frail, D. A., Weisberg, J. M., Cordes, J. M., & Mathers, C. 1994, *ApJ*, 436, 144.
- Hartmann, Dap and Burton, W.B. 1997, *Atlas of Galactic Neutral Hydrogen*

(Cambridge: Cambridge University Press).

Holberg, J.B. 1986, *Ap.J.*, 311, 969.

Kalberla, P. M. W., Mebold, U., & Reich, W. 1980, *A&A*, 82, 275.

Kalberla, P. M. W., Schwarz, U. J., & Goss, W. M. 1985, *A&A*, 144, 27.

Kulkarni, S. R. and Heiles, C. 1988, in *Galactic and Extragalactic Radio Astronomy*, eds. G. Verschuur and K. Kellerman (Heidelberg: Springer-Verlag), p. 95

McKee, C.F. and Ostriker, J.P. 1977, *Ap.J.*, 218, 148.

Mebold, U., & Hills, D. 1975, *A&A*, 42, 187.

Radhakrishnan, V., Goss, W. M., Murray, J. D., & Brooks, J. W. 1972, *ApJS*, 24, 49.

Wolfire, M.G., Hollenbach, D., McKee, C.F., Tielens, A.G., and Bakes, E.L. 1995, *Ap.J.*, 443, 152.

Table 1.

	A	B
	-67 to -76 km s <sup>-1</sup>	-36 to -40 km s <sup>-1</sup>
Optical Depth: NW	$6.8 \pm 1.9 \times 10^{-4}$	$6.0 \pm 2.0 \times 10^{-4}$
Optical Depth: SE	$11 \pm 1.9 \times 10^{-4}$	$11 \pm 2.0 \times 10^{-4}$
Mean Optical Depth	$8.9 \pm 1.9 \times 10^{-4}$	$8.5 \pm 2.0 \times 10^{-4}$
T <sub>B</sub> (Effelsberg)	$5.6 \pm 1$ K	$4.0 \pm 1$ K
T <sub>B</sub> (Dwingeloo)	$4.7 \pm 2$ K	$4.5 \pm 2$ K
Mean T <sub>B</sub>	$5.3 \pm 1$ K	$4.1 \pm 1$ K
T <sub>s</sub>	$6000 \pm 1700$ K	$4800 \pm 1600$ K

### Figure Captions

Figure 1 – A continuum image of Cygnus A at 1.4 GHz made using line-free channels from the WSRT observations. The total flux density is 1575 Jy. The contours are a geometric progression in the square root of two. The first level is 5 Jy/beam. Dotted contours are negative levels. The FWHM of the Gaussian restoring beam is  $30'' \times 15''$  with the major axis oriented north-south.

Figure 2 – The upper frame shows the HI absorption spectrum toward north-west peak of Cygnus A. The spectral resolution in this, and subsequent, spectra is  $1 \text{ km s}^{-1} \text{ channel}^{-1}$ . The spectrum has been converted to optical depth using the continuum surface brightness of 346 Jy/beam at the resolution of Figure 1. The velocity scale is LSR. The CNM-free velocity ranges are labeled ‘A’ and ‘B’. The lower frame shows the corresponding spectrum of the south-east peak, where the continuum surface brightness is 398 Jy/beam.

Figure 3 – The upper frame shows the HI absorption spectrum toward the north-west peak of Cygnus A, after subtracting the continuum surface brightness of 346 Jy/beam. The velocity scale is LSR. The lower frame shows the same spectrum converted to optical depth using the continuum surface brightness of 346 Jy/beam. The optical depth scale has been expanded to show low optical depth absorption. The CNM-free velocity ranges A and B are indicated.

Figure 4 – The upper frame shows the HI absorption spectrum toward the south-east peak of Cygnus A, after subtracting the continuum surface brightness of 398 Jy/beam. The velocity scale is LSR. The lower frame shows the same spectrum converted to optical depth using the continuum surface brightness of 398 Jy/beam. The optical depth scale has been expanded to show low optical depth absorption. The CNM-free velocity ranges A and B are indicated.

Figure 1

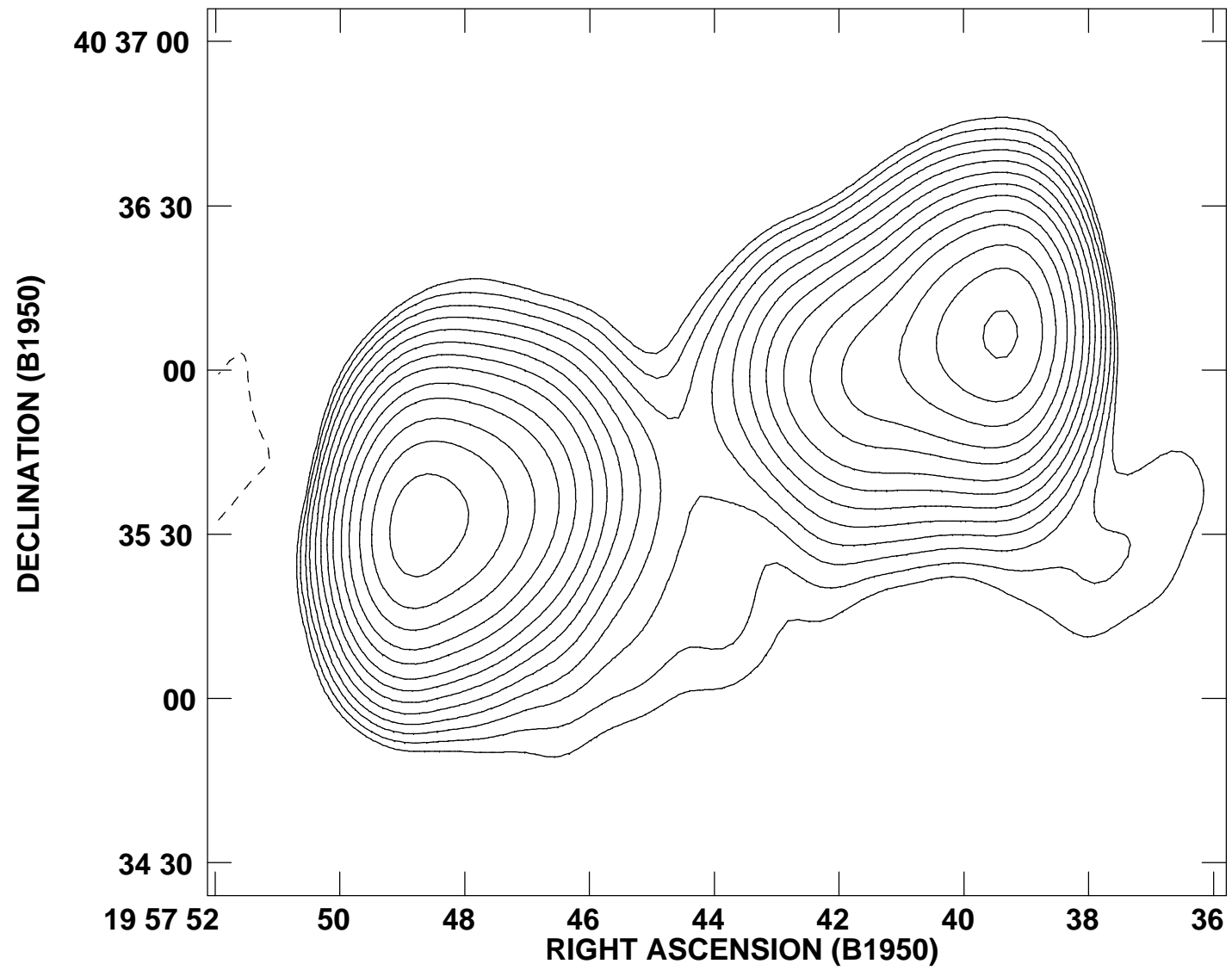




Figure 2

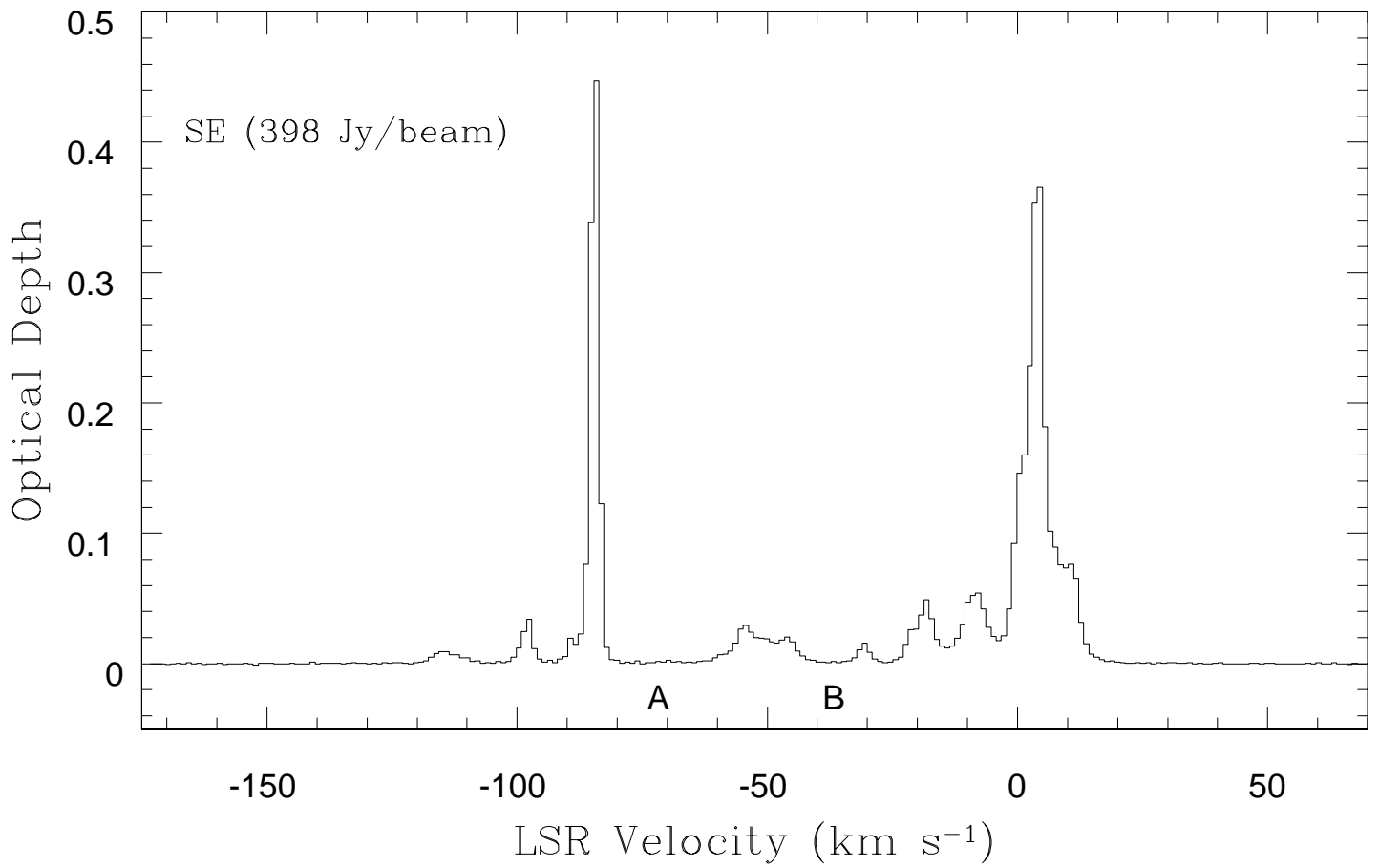
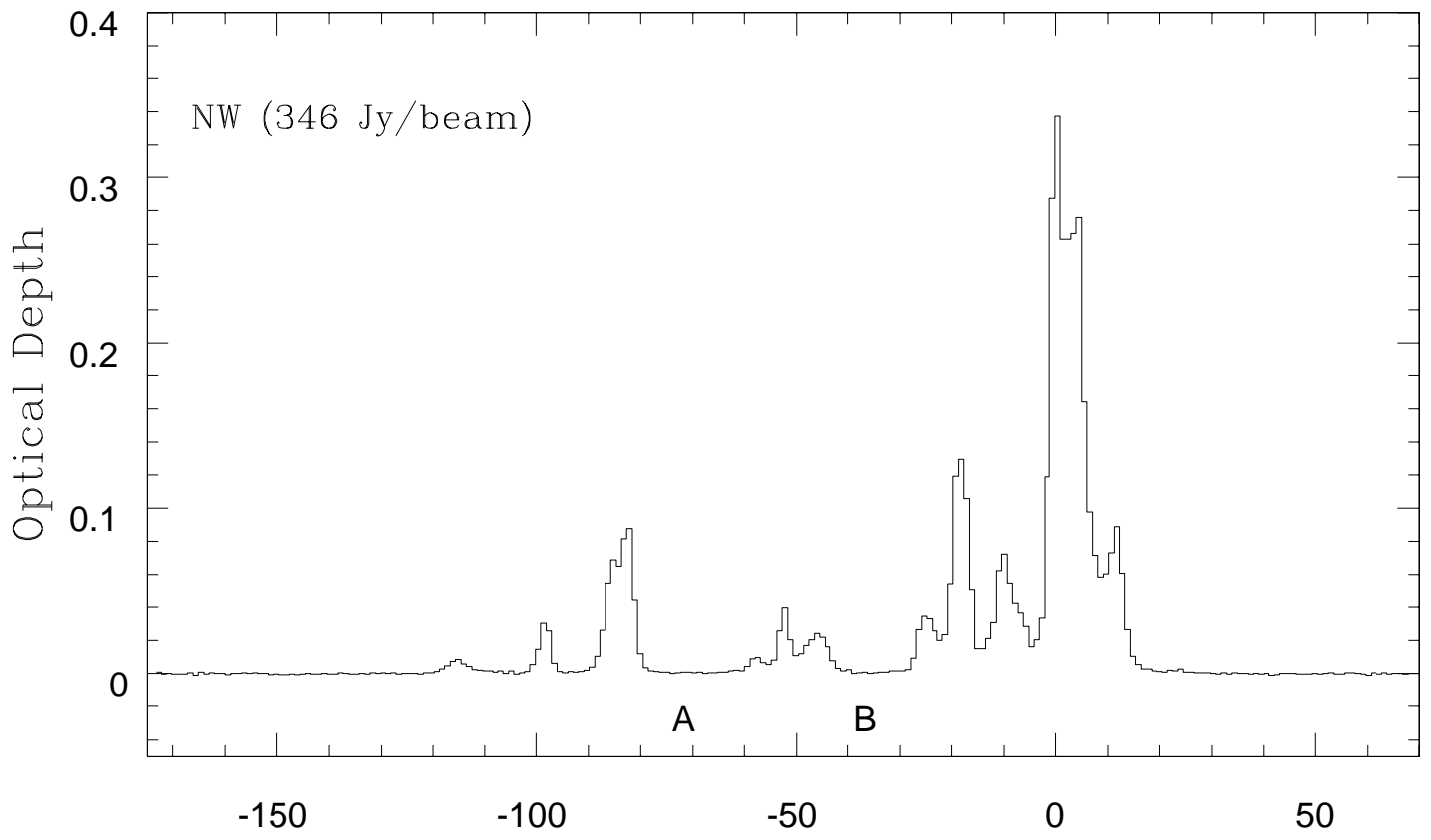


Figure 3 -- NW

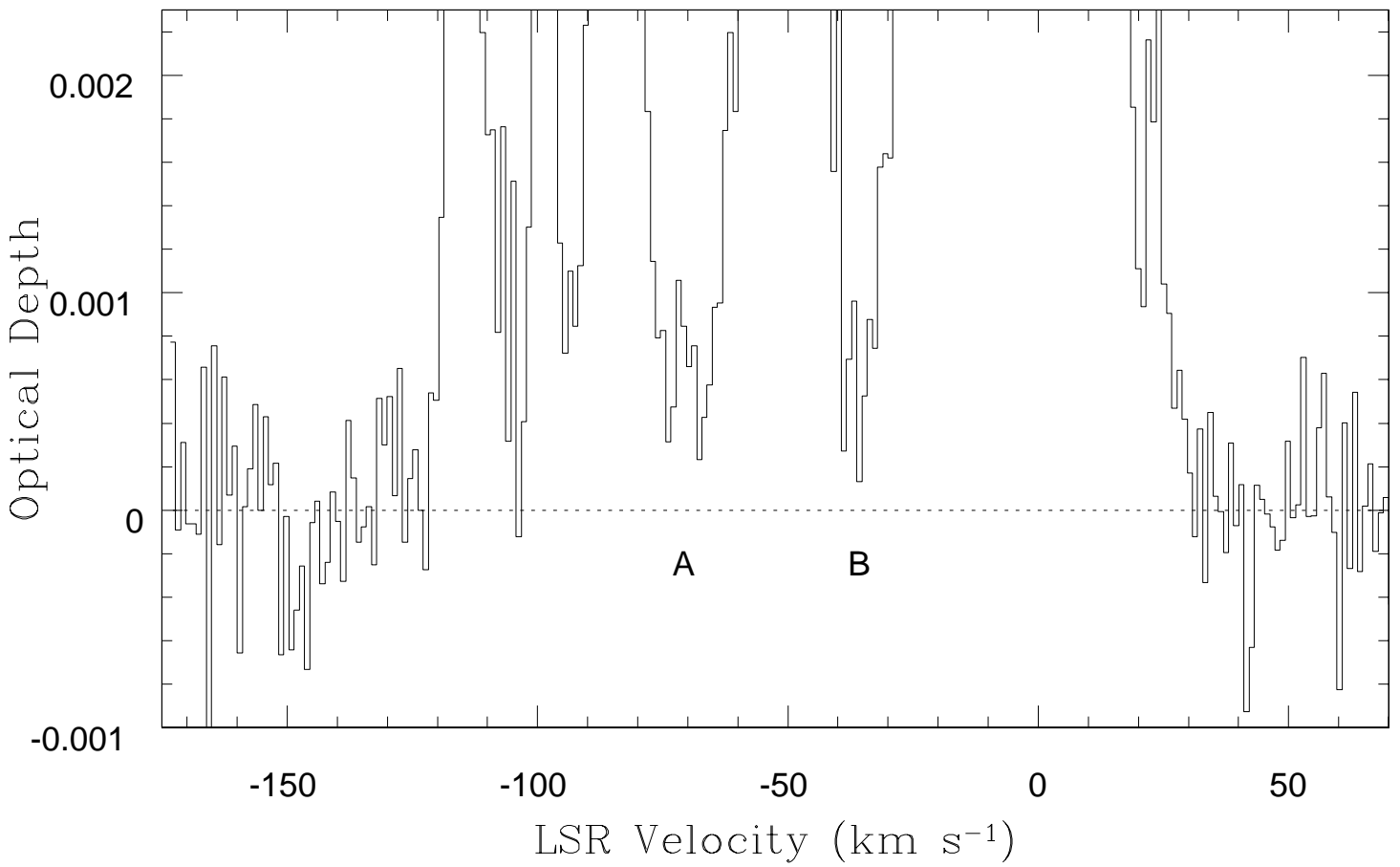
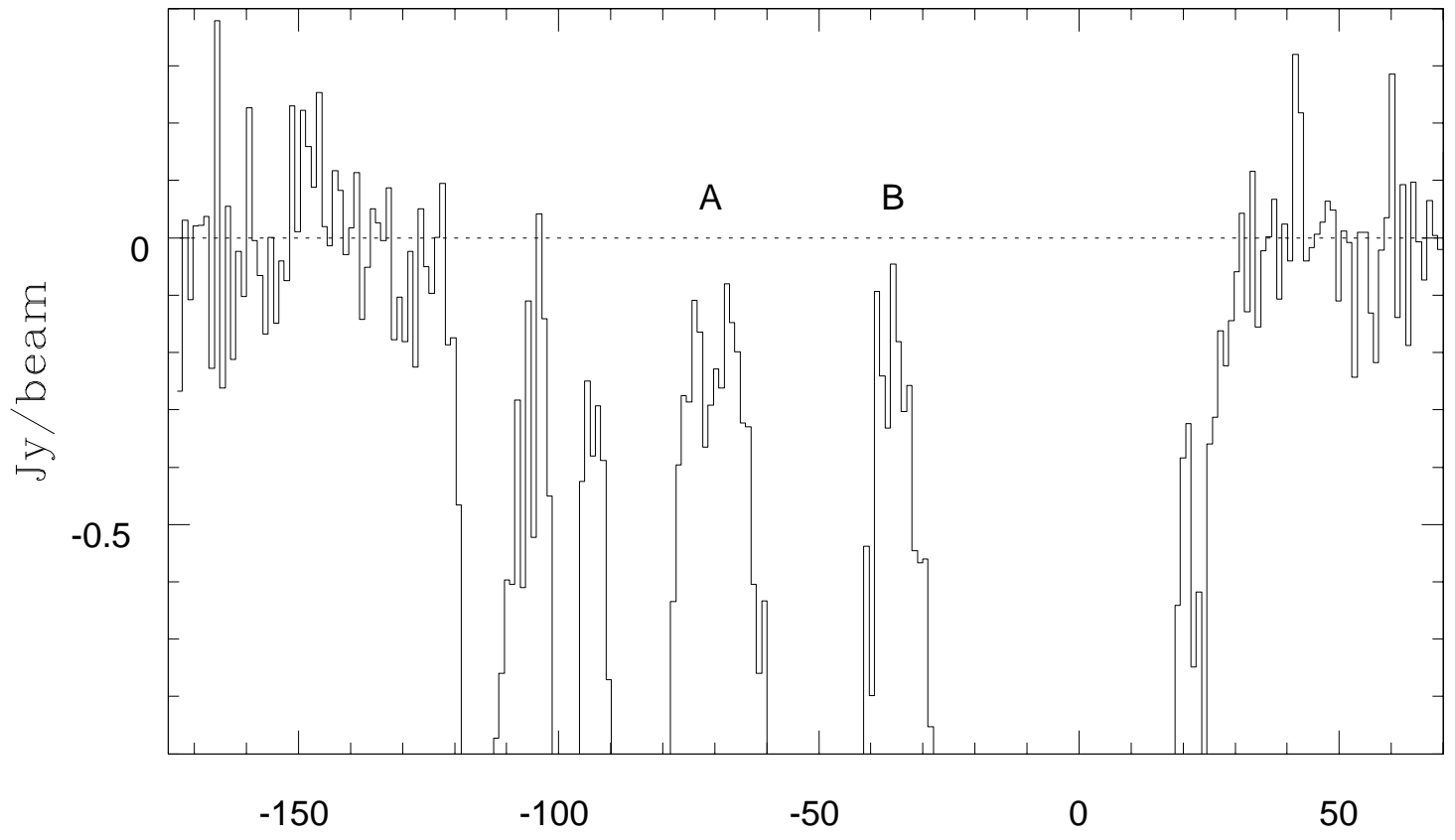


FIGURE 4 -- SE

